Journal of Power Sources 412 (2019) 294–300

Contents lists available at ScienceDirect

Journal of Power Sources

journal homepage: www.elsevier.com/locate/jpowsour

Impact of flow recirculation and anode dimensions on performance of a large scale microbial fuel cell

Ruggero Rossi[a], Patrick J. Evans[b], Bruce E. Logan[a,*]

[a] Department of Civil and Environmental Engineering, The Pennsylvania State University, University Park, PA, 16802, USA
[b] CDM Smith, Bellevue, WA, 98007, USA

HIGHLIGHTS

- Power density was 0.101 ± 0.006 W m^{-2} in an 85 L MFC fed domestic wastewater.
- Recirculating the anolyte increased the power density to 0.118 ± 0.006 W m^{-2}.
- A diagonal flow path across the electrodes produced the highest power densities.
- Reducing the anode brush diameter did not affect MFC performance.

ARTICLE INFO

Keywords:
MFC
Scaling up
Power density
Recirculation
HRT
Internal resistance

ABSTRACT

Many design and operational parameters that can impact power generation in microbial fuel cells (MFCs), such as flow over the electrodes, can only be effectively examined in larger-scale systems. A maximum power density of 0.101 ± 0.006 W m^{-2} (0.74 ± 0.05 W m^{-3}) was obtained in an 85-L MFC with graphite fiber brushes (5.1 cm diameter, 61 cm long) and flat air cathode (0.62 m^2 exposed area; anode-cathode spacing of 1.3 cm) in batch mode. Recirculating the anolyte diagonally through the chamber (entering the top right side of the reactor and exiting the bottom left side) further improved performance by 17% to 0.118 ± 0.006 W m^{-2}, at a hydraulic retention time (HRT) of 22 min (3.9 L min^{-1}), compared to static flow conditions. This power density was also higher than that obtained with parallel flow through the chamber (more evenly distributed using a manifold; 0.109 ± 0.009 W m^{-2}). Reducing the diameter of the anode brushes from 5.1 cm to 2.5 cm did not improve the anode performance. These results demonstrate the importance of electrode spacing and hydraulic flow on large-scale MFC performance.

1. Introduction

Microbial fuel cells (MFCs) use bacteria to directly produce electricity from biodegradable organic matter [1–4]. MFCs have great potential as a new method for wastewater treatment, in combination with further treatment processes such as an anaerobic fluidized bed membrane bioreactor (AFMBR) [3,5,6], to replace energy-intensive activated sludge processes. Application of MFCs for wastewater treatment requires that effective power generation and treatment efficiency be obtained with larger-scale reactors, operated under realistic conditions [1,2,7–10]. Most bench scale MFC studies have been conducted using relative optimal conditions for power generation, such as well-buffered phosphate buffer solutions (PBS) with high conductivities, and high concentrations of acetate as a substrate rather than unbuffered solution with low concentrations of complex organics in most domestic wastewaters [3,7,11,12]. Using small electrodes and favourable test conditions at more optimal temperatures (~30 °C), relative to wastewaters (typically < 25 °C), produces power densities much higher than those that could be obtained using low-strength wastewaters at typical municipal wastewater treatment facilities [3,11–13]. Thus, the performance of a large scale MFCs can only be tested by using larger electrodes, and operating the system with actual wastewaters [1,7,9,14].

Many design elements of MFCs have only been examined in smaller-scale reactors (1 L or much less), typically with single anodes and cathodes, and under static flow conditions [15]. The impact of the variation of different design parameters, such as electrode diameter, length and spacing from the cathode, have not been well examined in larger scale systems. A comparison of anode types based on reports in the literature showed that cylindrical brush anodes generally produced higher current densities than flat carbon felt, carbon cloth and carbon

* Corresponding author.
E-mail address: blogan@psu.edu (B.E. Logan).

https://doi.org/10.1016/j.jpowsour.2018.11.054
Received 15 August 2018; Received in revised form 30 October 2018; Accepted 16 November 2018
0378-7753/

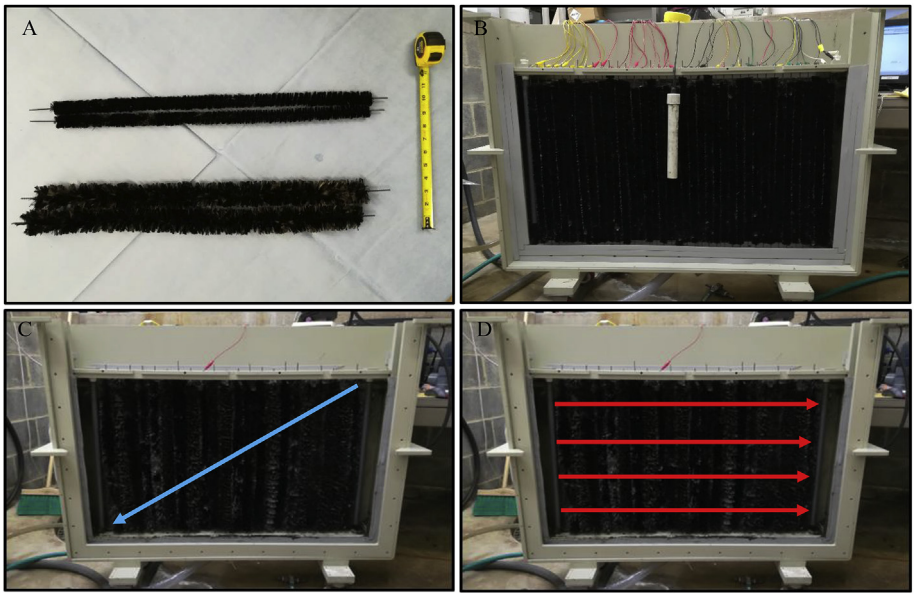

Fig. 1. Photos of (A) the two anode brushes (diameter of 2.5 cm (top) or 5.1 cm (bottom)) and (B) of the 38 anode brushes (diameter of 2.5 cm) installed in the MFC. (C) Diagonal and (D) parallel flow paths in the anodic chamber of the 85 L MFC with 22 anode brushes (diameter of 5.1 cm).

paper anodes, when coupled to a cathode with a platinum catalyst [16]. Graphite fiber brush anodes and activated carbon based cathodes have produced power densities up to 2.78 ± 0.08 W m^{-2} for small MFCs (0.028 L) fed with acetate in phosphate buffer solution (PBS 50 mM) [17], and up to 0.8 ± 0.03 W m^{-2} using domestic wastewater (primary clarifier effluent) [18]. The brushes used in most bioelectrochemical systems (BESs) have been of the order of few centimeters in length, for example only 2.5 cm in 28 mL MFCs [1], 12 cm in 6.1 L [13], or 20 cm in 90 L [19], so there is little information on systems with longer brush anodes. The impact of brush diameter on power production has also not been well examined. Reducing the diameter of the anode brushes from 2.5 cm to 0.8 cm in a 28 mL MFC produced similar performance, but only if the anode coverage of the cathode was not changed. The maximum power density decreased up to 32% (from 1000 to 680 mW m^{-2}) if the anode projected area was decreased by 80% [20]. In studies on larger MFCs (174 mL) fed acetate in PBS, reducing the diameter of the anode brushes from 2.5 cm to 0.8 cm increased the maximum power density under static (from 0.69 W m^{-2} to 1.03 W m^{-2}) and dynamic flow conditions (from 0.54 W m^{-2} to 1.02 W m^{-2}) [21]. However, in tests using wastewater, the reactor had unstable performance suggesting that the size of the brush anodes was too small, and the wastewater too dilute, to maintain sufficiently anaerobic conditions in the brush anodes [22].

Relatively few studies have examined the impact of the flow rate or recirculation on performance in large-scale MFCs [15,23–25]. In a 6.1-L modular MFC fed with domestic wastewater with 6 cathodes and 4 brush anode arrays switching from fed-batch to continuous flow decreased the maximum power density from 0.400 ± 0.008 W m^{-2} to 0.25 ± 0.02 W m^{-2} (HRT of 8 h) [13]. Serial flow (entering into one module and then moving successively through the four modules) or parallel flow (entering and exiting each individual module) mode produced similar average power densities with domestic wastewater (0.21 W m^{-2} with parallel flow, and 0.20 W m^{-2} in serial flow) [26]. Recirculating a buffered anolyte in a (4.9 L) MFC operated in upflow mode increased maximum power density and COD removal in long term tests compared to static flow conditions, but the tubular architecture was much different than other scalable flat-plate designs [27].

To examine the impact of recirculation flow rate, path, and the brush diameter, the performance of a larger-scale (85 L) MFC was investigated using domestic wastewater. Diagonal and parallel flow paths were chosen for the anolyte flow, each at two different HRTs, with performance examined for the anode and cathode potentials, and overall power densities. In order to better understand the effect of the brush diameter on liter-scale MFC performance, two brush diameters were compared in terms of maximum power generation. The electrode spacing and the anode projected area relative to the cathode was kept constant by using more brushes with smaller diameters and maintaining the same gap between the anode edge and the cathode.

2. Materials and methods

2.1. Electrode materials

Cathodes were 1.07 m long and 0.64 m in height with a total projected area of 0.68 m^2 and an exposed area of 0.62 m^2 [9]. This large cathode was constructed based on a “window pane” approach by using a single stainless steel sheet that contained 15 cathodes (panes). Each of the cathode sheets (VITO CORE®, Mol, Belgium) were made by pressing together a mixture of activated carbon (AC; 70–90 wt%; Norit SX plus, Norit Americas Inc., TX) and polytetrafluoroethylene (PTFE) binder, onto a stainless steel mesh current collector. A PTFE diffusion layer (70% porosity) was then added on top of the catalyst layer which became the air-side of the cathode [28]. The cathode sheets were welded into laser cut holes (“window panes”) in the stainless steel frame to allow the cathode sheets to be exposed to the anolyte on one side, and air on the other side. The cathode was periodically cleaned to minimize changes in performance over time due to cathode fouling [29].

Two different brush anodes sizes were used in the present study all made from graphite fiber (PANEX 35 50K, Zoltek) wound between two titanium wires, 5.1 cm in diameter and 61 cm long from a previous MEC configuration (Gordon Brush, CA, USA) (Fig. 1) [30] and 2.5 cm in diameter and 61 cm long. All anodes were heat treated at 450 °C in air for 30 min prior to use in MFCs [31].

2.2. Pilot-scale reactor

The MFC was a custom rectangular tank (1.1 m long, 0.15 m wide and 0.85 m height) as previously described [9]. The tank had a bracket slot 10 cm from the wall of the water side, where the cathode was attached to form the anolyte chamber. The cathodes were secured to the frame with 25 screws using a plastic U-shape fastener and a gasket (closed cell PVC vinyl foam), producing a cathode specific surface area

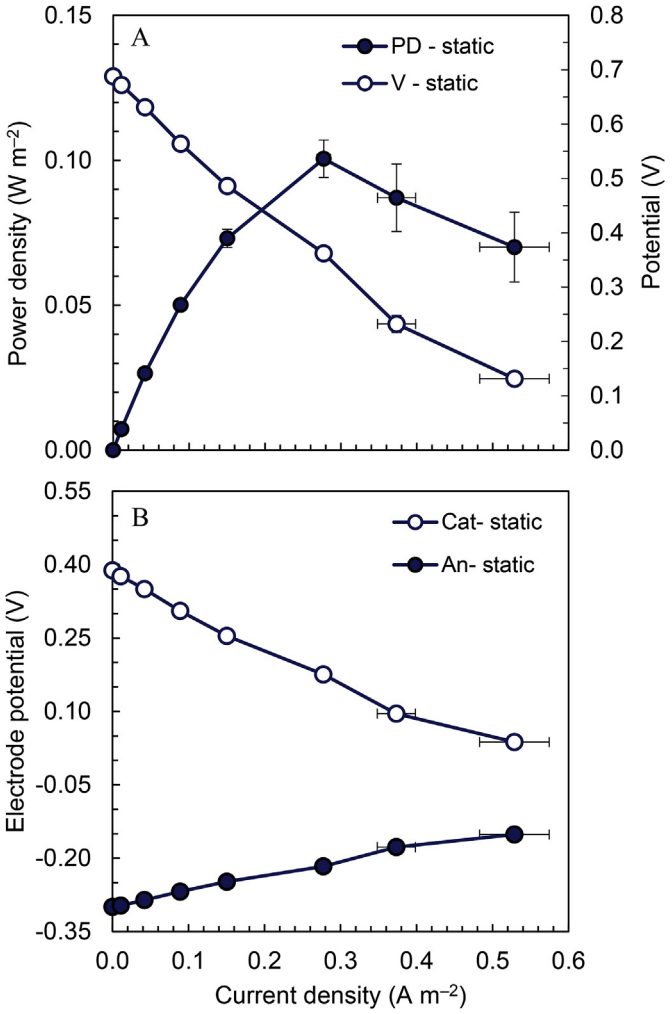

Fig. 2. (A) Power density curve and whole cell potential and (B) correspondent cathode (Cat) and anode (An) potentials using 22 anode brushes (D = 5.1 cm, projected area = 0.60 m^2) in the anode module under static conditions.

of 7.3 m^2 per m^3 of anolyte volume. This low specific area of the cathode due to the relatively larger width of the tank compared to previous designs (25 m^2 m^{-3}, width 4 cm, 28 mL [1], 29 m^2 m^{-3}, width 6 cm, 1.4 L [11]), was used here to accommodate large diameter anode brushes, a reference electrode, and to easily inspect the condition of the electrodes. The cathode air chamber was formed by sliding a sheet of PVC into a slotted groove 5 cm from the cathode. To reduce the cathode deformation due to the pressure of the water on the cathode, the space between the clear PVC sheet and the cathode was filled with 19 spacers [32,33], constructed by rolling polypropylene mesh (XN3110-48P, Industrial Netting, USA) into tubes (4 cm diameter by 1 m long), with the rolled tubes held together using zip ties.

An anode module made with a polyvinyl chloride (PVC) frame was constructed to produce a linear array of graphite fiber brushes. The PVC module held 22 (D = 5.1 cm) or 38 (D = 2.5 cm) brushes (as indicated), with the ends of the brushes secured at the top and bottom of the module. The brush module was placed parallel to the cathode, in the middle of the anode chamber, producing a distance of 1.3 cm between the edge of the anode brushes and the cathode surface [21]. The anodes were connected in parallel to the circuit by an external single titanium wire. To avoid short circuiting between the electrodes, and to reduce biofilm growth on the cathode, the reactors were operated with a cloth separator (PZ-1212, Contec, USA) placed on the water side of the cathode [34,35].

2.3. Microbial fuel cell tests

The MFC operated at room temperature in a laboratory at the Pennsylvania State University Wastewater Treatment Plant in order to feed it directly with fresh primary clarifier effluent wastewater (WW). Total and soluble COD were measured using method 5220 (Hach COD system, Hach Company, Loveland, Colorado). The Coulombic efficiency was calculated as previously defined [36]. The acclimation of the MFC for power generation was previously described [9], based on feeding the reactor domestic wastewater in fed-batch operation over several weeks. Single cycle polarization tests were conducted by feeding the reactor with fresh wastewater and maintaining the system at open circuit conditions for 2 h, and then varying the external resistance from 100 to 25, 10, 5, 2, 1 and 0.4 Ω at 20 min intervals.

The current was calculated based on the voltage (U) across the external resistor, and recorded using a computer based data acquisition system (2700, Keithley Instrument, OH). Current densities (i) and power densities (P) were normalized to the total exposed cathode area (A = 0.62 m^2) and calculated as $i = U/RA$ and $P = iU$, where R is the external resistance. The presence of the stainless steel frame in the cathode reduced the active area of the electrode. Therefore, the power density was also reported in terms of the active area ($_{AA}$ = 0.47 m^2) of the cathode (P_{AA} = iU/$_{AA}$) [37]. During each polarization test, the anode potential was recorded using an immersion reference electrode (RE, Electrochemical Devices Inc., OH; + 0.199 V vs. SHE), kept close to the cathode and in the same position for all the tests. The cathode potential (E_{Cat}) was estimated using the cell voltage as $E_{Cat} = U + E_{An}$. The anode and the cathode potentials were corrected based on the conductivity of the solution and the distance from the RE [38]. The distance anode-RE was 1.2 cm while the spacing between the cathode and the RE was 0.1 cm. The average conductivity of the wastewater at 25 °C was 1.2 mS cm^{-1}. The measured electrode potentials (not corrected for conductivity) are reported in the Supporting Information. The internal resistance was calculated as:

$$R_{int} = \sqrt{\frac{OCV^2\, R_{ext}}{P_{max}}} - R_{ext} \quad (1)$$

where R_{int} is the calculated internal resistance, OCV is the open circuit voltage, R_{ext} is the external resistance at the maximum power density (P_{max}) [36].

2.4. Impact of anolyte recirculation

The impact of fluid flow was examined by recirculating the anolyte within the module. A diagonal flow path through the modules (entering the top right side of the reactor and exiting the bottom left side) and a parallel flow path (using a manifold to distribute the flow across the height of the module) were applied at two different hydraulic retention time (HRT) for a single pass of 77 and 22 min (Fig. 1). The flow rates were 3.9 L per minute (L min^{-1}) (HRT 22 min) and 1.1 L min^{-1} (HRT 77 min).

3. Results and discussion

3.1. Power production in static conditions

The maximum power density based on single cycle polarization tests of the MFC was 0.101 ± 0.006 W m^{-2} (Fig. 2A). Normalizing the produced power by the active area of the cathode (0.47 m^2) resulted in a maximum power density of P_{AA} = 0.133 W m^{-2}. The whole cell OCV was 0.688 ± 0.003 V, and the potential decreased to 0.36 ± 0.01 V at the maximum power density. The electrode potential drop between OCV and 0.53 ± 0.05 A m^{-2} was |0.350 V| for the cathode and |0.149 V| for the anode. This potential drop is large compared to that obtained in smaller MFCs fed domestic wastewater. For example, the

same cathode material at a similar electrode spacing (1.4 cm) in a 28 mL MFC fed with domestic wastewater produced a cathode potential drop of |0.166 V|, but over a much larger current density range that reached as high as 1.9 ± 0.1 A m^{-2}. The anode potential decreased by about the same amount for the same current density region of |0.151 V| [9]. The larger difference for the cathode indicated that in this system the cathode was primarily limiting power production. The anode potential at the maximum power density was – 0.217 ± 0.005 V at 0.277 ± 0.009 A m^{-2} and the cathodic potential was 0.176 ± 0.006 V at the same current density.

The power density using an electrode spacing between anode and cathode of 1.3 cm was 22% greater than that previously obtained with an electrode spacing of 3.5 cm in the same MFC (0.083 ± 0.006 W m^{-2}) [9]. The higher power density here with less electrode spacing was due to a decrease in the internal resistance from 2.19 Ω for the larger spacing compared to 1.88 Ω here (eq. (1). Of this calculated decrease of 0.31 Ω, it is estimated that 0.30 Ω was due to the decrease in the solution resistance (from 0.47 Ω to 0.17 Ω, calculated at an electrode spacing of 3.5 cm and 1.3 cm with a solution conductivity of 1.2 mS cm^{-1}) [36,38]. Additional tests were conducted with a reduced number of brushes (8 brushes) at 1.3 cm electrode spacing. The maximum power density was 0.068 ± 0.002 W m^{-2}, which was only 10% higher than that obtained with an electrode spacing of 3.5 cm and 8 brushes in previous tests (0.061 ± 0.003 W m^{-2}) [9]. Raw data and internal resistance calculations are reported in the Supporting Information.

3.2. Recirculation with a diagonal flow path

When the MFC was operated at the shortest theoretical HRT of 22 min the maximum power density based on polarization data was 0.118 ± 0.006 W m^{-2} (P_{AA} = 0.156 W m^{-2}) (Fig. 3). Increasing the HRT to 77 min reduced the performance of the MFC and the power density decreased to 0.106 ± 0.008 W m^{-2} (P_{AA} = 0.140 W m^{-2}) (Fig. 3). The maximum power density increased by 17% with an HRT of 22 min, and by only 5% with an HRT of 77 min, compared to that obtained under static flow conditions (0.101 ± 0.006 W m^{-2}).

Recirculating the anolyte reduced the anodic overpotential making the anode potential more negative. For example, the anode potential was – 0.242 ± 0.006 V (0.301 ± 0.008 A m^{-2}) at the maximum power density with an HRT of 22 min, with a more positive potential of – 0.224 ± 0.008 V (0.28 ± 0.01 A m^{-2}) at an HRT of 77 min. These are both better (more negative potentials) than that produced with no recirculation (– 0.217 ± 0.005 V, 0.277 ± 0.009 A m^{-2}). The cathodic potentials were similar for all operational modes at the maximum power densities (0.18 ± 0.01 V, HRT 22 min; 0.18 ± 0.02 V, HRT 77 min; and 0.17 ± 0.01 V static condition) with only small differences at current densities above 0.35 A m^{-2}.

3.3. Recirculation with a parallel flow path

Recirculating the anolyte in a parallel flow path across the electrodes resulted in performance similar to that obtained with static flow conditions (Fig. 4). The maximum power density was 0.109 ± 0.009 W m^{-2} (P_{AA} = 0.144 W m^{-2}) with the highest flow rate (HRT of 22 min) in respect to 0.101 ± 0.006 W m^{-2} obtained in static conditions, and 0.100 ± 0.006 W m^{-2} (P_{AA} = 0.132 W m^{-2}) with the lowest HRT of 77 min. These maximum power densities were both slightly lower than that produced at the same HRT using a diagonal flow path (8% lower at 22 min HRT and 6% lower at 77 min HRT). The lower power densities in the parallel flow rate tests were due to changes in both the anode and cathode overpotentials compared to the diagonal flow rate tests. For example, in the parallel flow rate, the anode potentials at the maximum power densities were – 0.236 ± 0.005 V (HRT 22 min) and – 0.24 ± 0.01 V (HRT 77 min), while the cathode potentials were 0.17 ± 0.01 V (HRT 22 min) and 0.15 ± 0.02 V (HRT 77 min).

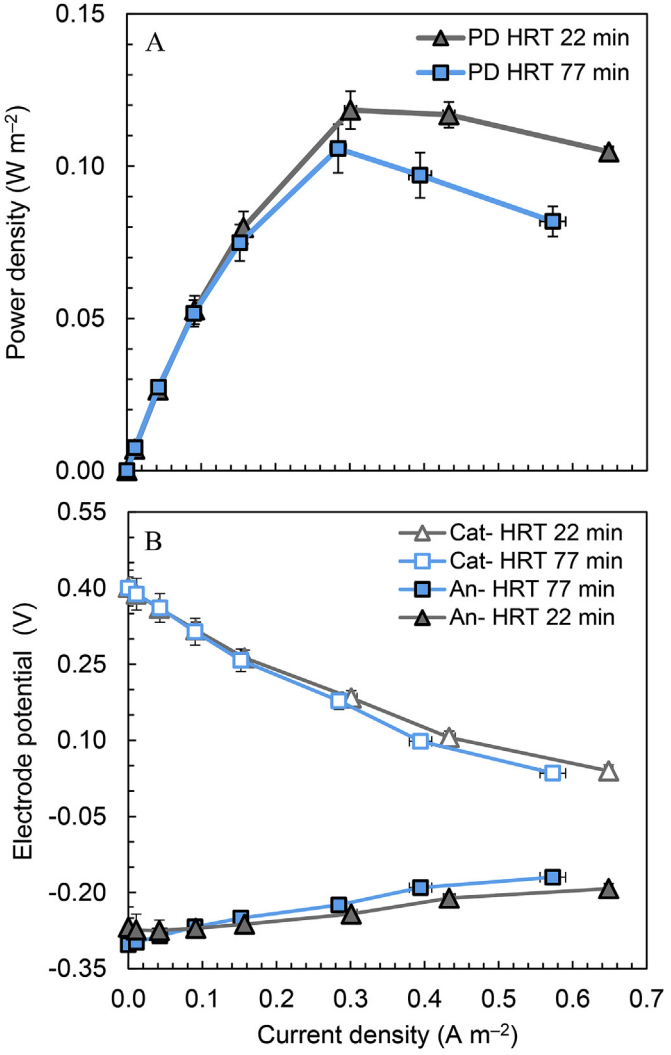

Fig. 3. (A) Power density curves and (B) correspondent cathode (Cat) and anode (An) potentials at an HRT of 22 min or 77 min in "diagonal" flow path.

The small differences in the maximum power densities between the diagonal and the parallel flow rate could also be due to slight differences in the wastewater characteristics. The COD in the parallel flow rate tests was 530 ± 38 mg L^{-1} (HRT 77 min) and 444 ± 68 mg L^{-1} (HRT 22 min), compared to slightly lower CODs at these HRTs in the diagonal tests of 465 ± 14 mg L^{-1} (HRT 77 min) and 338 ± 24 mg L^{-1} (HRT 22 min). The differences could also be due to cathode fouling. The polarization tests for the parallel flow rates were conducted after those in diagonal flow mode, and thus the slightly more negative cathode potentials at the maximum power densities could have been due to cathode aging or fouling.

3.4. Impact of brush diameter on MFC performance

To evaluate if reducing the brush diameter could improve the MFC performance, the 22 anode brushes of 5.1 cm diameter were replaced with 38 anode brushes of 2.5 cm diameter (to maintain full cathode coverage), with the same brush-edge to cathode spacing of 1.3 cm (Fig. 5). Following the anodes acclimation (one month) the maximum power density produced with 38 anode brushes was 0.089 ± 0.003 W m^{-2} in the non-recirculation flow (static) condition. This was 18% lower than the maximum power density obtained with larger anodes due to an increase in the internal resistance of the MFC.

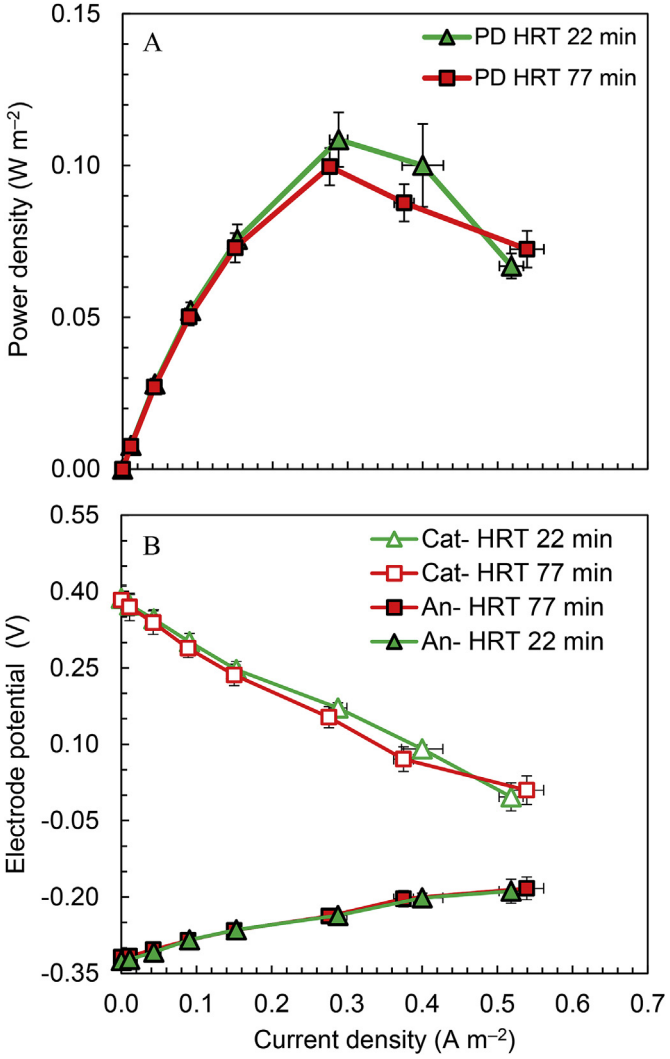

Fig. 4. (A) Power density curves and (B) correspondent cathode (Cat) and anode (An) potentials at an HRT of 22 min or 77 min in "parallel" flow path.

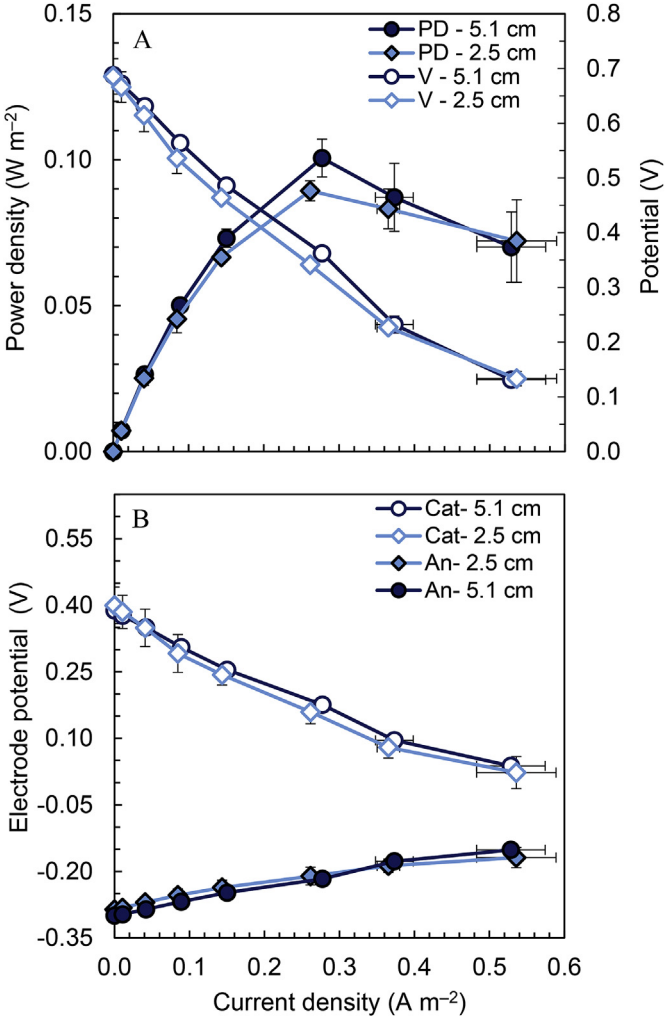

Fig. 5. (A) Power density curves and (B) correspondent cathode (Cat) and anode (An) potentials with anode brushes of 2.5 and 5.1 cm diameter.

The lower power output of the MFC with smaller anodes was primarily due to a decrease in the cathode potential. The cathode potential at the maximum power density was 0.159 ± 0.002 V, which corresponds to a 10% decrease compared to polarization tests with larger anodes under the same conditions (0.176 ± 0.007 V). The anode potentials at the maximum power density were similar for smaller (– 0.21 ± 0.02 V) and larger (– 0.22 ± 0.01 V) anodes. The decrease in the cathode performance was likely due to cathode fouling [35], since the cathode was in operation for one additional month compared to the previous tests with the larger anodes. Thus, we concluded that reducing the diameter of the brushes from 5.1 cm to 2.5 cm did not alter the anode performance in static flow conditions.

Polarization data were also obtained using the smaller diameter brushes with recirculation in the diagonal flow direction, at the two HRTs (Fig. 6). The maximum power densities increased by 24% to 0.11 ± 0.01 W m^{-2} (HRT 77 min), and by 17% to 0.104 ± 0.008 W m^{-2} (HRT 22 min) compared to static flow conditions. Cathode potentials were unaffected by the different HRTs (0.17 ± 0.02 V at 77 min, and 0.19 ± 0.01 V at 22 min). The difference in power densities was therefore due to differences in the anode potentials (– 0.211 ± 0.001 V at an HRT of 22 min, compared to – 0.234 ± 0.004 V at an HRT of 77 min). Thus, the higher power output at the HRT of 77 min was in part due to the differences in the average COD concentrations, as the influent COD was 22% higher at the highest HRT of 77 min (509 ± 42 mg L^{-1}) in respect to the lowest HRT of 22 min (417 ± 48 mg L^{-1}).

The maximum power density of the 85 L MFC with 5.1 cm diameter brushes in diagonal flow path (HRT 22 min) was 0.118 ± 0.006 W m^{-2}, or about one third of that reported for small chamber MFCs (0.304 ± 0.009 W m^{-2}, 28 mL, brush anode, VITO cathode) fed with domestic wastewater [9]. The decrease in power output was mainly due to the lower cathode performance [9], it has been previously shown that the impact of the higher water pressure on the electrodes decreases the effective surface area of the cathode catalyst in contact with the air [39,40], and that a large electrode had a higher ohmic resistance due to the low electrical conductivity of the carbonaceous catalysts [41]. Moreover, the stainless steel frame decreased the exposed area of the cathode by 23%, and so normalizing the maximum power output to the active area resulted in a higher power density of P_{AA} = 0.133 W m^{-2}. Therefore, connecting two cathodes to one anode array should further increase the maximum power output of the MFC. For example, doubling the cathode surface area from 290 cm^2 to 580 cm^2 in a fed-batch 1.6 L MFC increased the volumetric power density from 3.5 W m^{-3} to 6.8 W m^{-3} [42]. With continuous flow and an HRT of 2.2 h in another study, the maximum power in polarization tests increased by 39% (from 1.20 mW to 1.67 mW) by connecting two cathodes on either sides of the brush array [15].

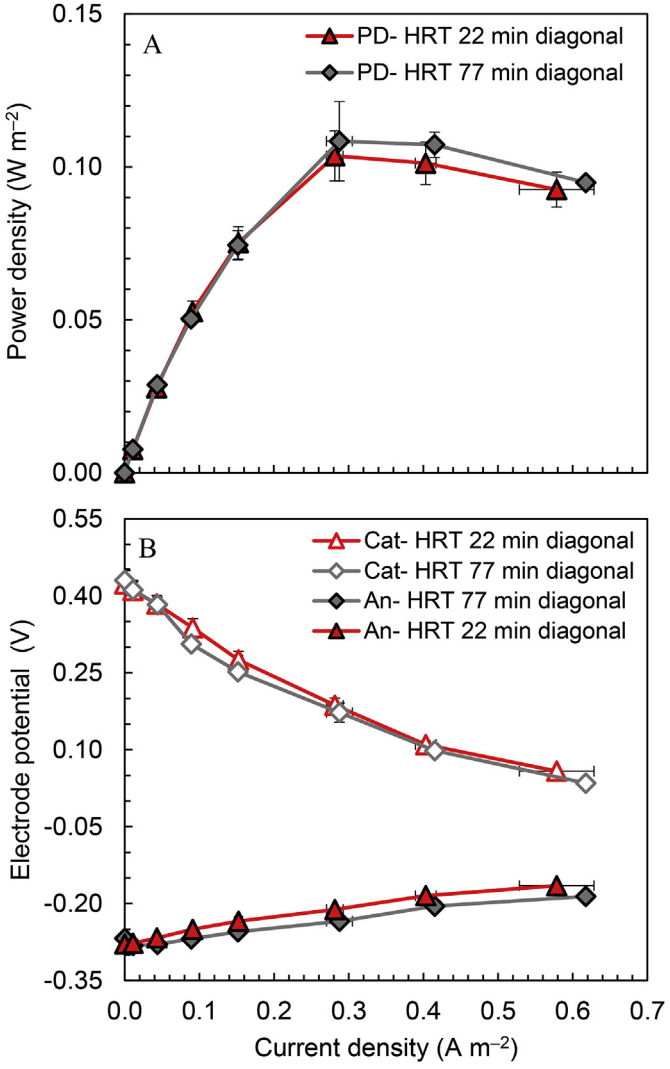

Fig. 6. (A) Power density curves and (B) correspondent cathode (Cat) and anode (An) potentials with 38 anode brushes and at an HRT of 22 min or 77 min in "diagonal" flow path.

3.5. COD removal and Coulombic efficiency

The MFC with 2.5 cm diameter brushes had a COD removal of 82% in 10 days, from 428 ± 7 mg L^{-1} to 79 ± 6 mg L^{-1}, which was similar to that of the MFC with the larger brush anodes (D = 5.1 cm, COD removal 80%) in static conditions [9]. When anolyte was recirculated in a diagonal flow path, the COD removal slightly decreased to 79% removal in 4 days (HRT 77 min, COD from 544 ± 11 mg L^{-1} to 114 ± 2 mg L^{-1}), and to 69% in only 1 day (HRT 22 min, COD from 468 ± 1 mg L^{-1} to 144 ± 4 mg L^{-1}). In parallel flow path the COD removal was 79% in 4 days (HRT 77 min, COD from 639 ± 2 mg L^{-1} to 162 ± 3 mg L^{-1}) and 68% in 1 day (HRT 22 min, COD from 493 ± 4 mg L^{-1} to 157 ± 9 mg L^{-1}).

The CE based on conversion of COD to current was 21% in static conditions (27% with 5.1 cm diameter brushes [9]) but it decreased to only 7% (HRT 77 min) and 2% (HRT 22 min) in dynamic flow conditions with a diagonal flow path. Similar CEs were obtained in parallel flow path (6% with HRT of 77 min and 3% with HRT of 22 min). This finding that the COD was removed faster with recirculation indicated that flow past the cathode increased the rate of oxygen transport into the wastewater. It has been previously shown that decreasing the HRT in an MFC decreases the final CE [15]. The CE obtained here in static condition is similar to the 22% previously achieved in small chamber MFC fed with domestic wastewater at low external resistance (100 Ω), which also had static conditions [5].

4. Conclusions

A maximum power density of 0.101 ± 0.006 W m^{-2} was obtained using the 85-L MFC with a cathode projected area of 0.62 m^2 in static flow conditions (1.3-cm electrode spacing). Recirculating the anolyte over the electrodes in a diagonal direction increased the maximum power density by 17% to 0.118 ± 0.006 W m^{-2} at an HRT of 22 min, but only by 5% to 0.106 ± 0.008 W m^{-2} at a longer HRT of 77 min, compared to static flow conditions. The reason for the increase was primarily due to reduced anodic overpotentials. Reducing the diameter of the anode brushes from 5.1 cm to 2.5 cm, while maintaining the same distance of the edge of the anode brush to the cathode, did not impact anode overpotentials. Therefore, the decrease in maximum power output (0.089 ± 0.003 W m^{-2}) for tests with different brush diameters was due to a change in the performance of the cathode, and not the anodes.

Acknowledgments

The research was supported by funds provided by the Environmental Security Technology Certification Program via cooperative research agreement W9132T-16-2-0014 through the US Army Engineer Research and Development Center.

Appendix A. Supplementary data

Supplementary data to this article can be found online at https://doi.org/10.1016/j.jpowsour.2018.11.054.

References

[1] B.E. Logan, M.J. Wallack, K.Y. Kim, W. He, Y. Feng, P.E. Saikaly, Assessment of microbial fuel cell configurations and power densities, Environ. Sci. Technol. Lett. 2 (2015) 206–214, https://doi.org/10.1021/acs.estlett.5b00180.
[2] W.-W. Li, H.-Q. Yu, Z. He, Towards sustainable wastewater treatment by using microbial fuel cells-centered technologies, Energy Environ. Sci. 7 (2013) 911–924, https://doi.org/10.1039/C3EE43106A.
[3] F. Zhang, Z. Ge, J. Grimaud, J. Hurst, Z. He, Long-term performance of liter-scale microbial fuel cells treating primary effluent installed in a municipal wastewater treatment facility, Environ. Sci. Technol. 47 (2013) 4941–4948, https://doi.org/10.1021/es400631r.
[4] E.M. Milner, K. Scott, I.M. Head, T. Curtis, E.H. Yu, Evaluation of porous carbon felt as an aerobic biocathode support in terms of hydrogen peroxide, J. Power Sources 356 (2017) 459–466, https://doi.org/10.1016/j.jpowsour.2017.03.079.
[5] X. Zhang, W. He, L. Ren, J. Stager, P.J. Evans, B.E. Logan, COD removal characteristics in air-cathode microbial fuel cells, Bioresour. Technol. 176 (2015) 23–31, https://doi.org/10.1016/j.biortech.2014.11.001.
[6] L. Ren, Y. Ahn, B.E. Logan, A two-stage microbial fuel cell and anaerobic fluidized bed membrane bioreactor (MFC-AFMBR) system for effective domestic wastewater treatment, Environ. Sci. Technol. 48 (2014) 4199–4206, https://doi.org/10.1021/es500737m.
[7] E.S. Heidrich, S.R. Edwards, J. Dolfing, S.E. Cotterill, T.P. Curtis, Performance of a pilot scale microbial electrolysis cell fed on domestic wastewater at ambient temperatures for a 12month period, Bioresour. Technol. 173 (2014) 87–95, https://doi.org/10.1016/j.biortech.2014.09.083.
[8] J. An, J. Sim, H.S. Lee, Control of voltage reversal in serially stacked microbial fuel cells through manipulating current: significance of critical current density, J. Power Sources 283 (2015) 19–23, https://doi.org/10.1016/j.jpowsour.2015.02.076.
[9] R. Rossi, D. Jones, J. Myung, E. Zikmund, W. Yang, Y. Alvarez, D. Pant, P.J. Evans, M.A. Page, D.M. Cropek, B.E. Logan, Evaluating a multi-panel air cathode through electrochemical and biotic tests, Water Res. 148 (2019) 51–59, https://doi.org/10.1016/j.watres.2018.10.022.
[10] Z. Ge, Z. He, Long-term performance of a 200 liter modularized microbial fuel cell system treating municipal wastewater: treatment, energy, and cost, Environ. Sci. Water Res. Technol. 2 (2016) 274–281, https://doi.org/10.1039/c6ew00020g.
[11] Y. Ahn, M.C. Hatzell, F. Zhang, B.E. Logan, Different electrode configurations to optimize performance of multi-electrode microbial fuel cells for generating power or treating domestic wastewater, J. Power Sources 249 (2014) 440–445, https://doi.org/10.1016/j.jpowsour.2013.10.081.
[12] E.S. Heidrich, J. Dolfing, M.J. Wade, W.T. Sloan, C. Quince, T.P. Curtis, Temperature, inocula and substrate: contrasting electroactive consortia, diversity and performance in microbial fuel cells, Bioelectrochemistry 119 (2018) 43–50,

https://doi.org/10.1016/j.bioelechem.2017.07.006.
[13] W. He, X. Zhang, J. Liu, X. Zhu, Y. Feng, B.E. Logan, Microbial fuel cells with an integrated spacer and separate anode and cathode modules, Environ. Sci. Water Res. Technol. 2 (2016) 186–195, https://doi.org/10.1039/c5ew00223k.
[14] H. Liu, S. Cheng, L. Huang, B.E. Logan, Scale-up of membrane-free single-chamber microbial fuel cells, J. Power Sources 179 (2008) 274–279, https://doi.org/10.1016/j.jpowsour.2007.12.120.
[15] K.Y. Kim, W. Yang, B.E. Logan, Impact of electrode configurations on retention time and domestic wastewater treatment efficiency using microbial fuel cells, Water Res. 80 (2015) 41–46, https://doi.org/10.1016/j.watres.2015.05.021.
[16] W. Yang, K.Y. Kim, P.E. Saikaly, B.E. Logan, The impact of new cathode materials relative to baseline performance of microbial fuel cells all with the same architecture and solution chemistry, Energy Environ. Sci. 10 (2017) 1025–1033, https://doi.org/10.1039/c7ee00910k.
[17] R. Rossi, W. Yang, L. Setti, B.E. Logan, Assessment of a metal–organic framework catalyst in air cathode microbial fuel cells over time with different buffers and solutions, Bioresour. Technol. 233 (2017) 399–405, https://doi.org/10.1016/j.biortech.2017.02.105.
[18] W. Yang, B.E. Logan, Immobilization of a metal – nitrogen – carbon catalyst on activated carbon with enhanced cathode performance in microbial fuel cells, ChemSusChem 9 (2016) 2226–2232, https://doi.org/10.1002/cssc.201600573.
[19] Y. Dong, Y. Qu, W. He, Y. Du, J. Liu, X. Han, Y. Feng, A 90-liter stackable baffled microbial fuel cell for brewery wastewater treatment based on energy self-sufficient mode, Bioresour. Technol. 195 (2015) 66–72, https://doi.org/10.1016/j.biortech.2015.06.026.
[20] V. Lanas, B.E. Logan, Evaluation of multi-brush anode systems in microbial fuel cells, Bioresour. Technol. 148 (2013) 379–385, https://doi.org/10.1016/j.biortech.2013.08.154.
[21] V. Lanas, Y. Ahn, B.E. Logan, Effects of carbon brush anode size and loading on microbial fuel cell performance in batch and continuous mode, J. Power Sources 247 (2014) 228–234, https://doi.org/10.1016/j.jpowsour.2013.08.110.
[22] J.L. Stager, X. Zhang, B.E. Logan, Addition of acetate improves stability of power generation using microbial fuel cells treating domestic wastewater, Bioelectrochemistry 118 (2017) 154–160, https://doi.org/10.1016/j.bioelechem.2017.08.002.
[23] B. Min, B.E. Logan, Continuous electricity generation from domestic wastewater and organic substrates in a flat plate microbial fuel cell, Environ. Sci. Technol. 38 (2004) 5809–5814, https://doi.org/10.1021/es0491026.
[24] S. Puig, M. Serra, M. Coma, M.D. Balaguer, J. Colprim, Simultaneous domestic wastewater treatment and renewable energy production using microbial fuel cells (MFCs), Water Sci. Technol. 64 (2011) 904–909, https://doi.org/10.2166/wst.2011.401.
[25] J.R. Kim, H.C. Boghani, N. Amini, K.F. Aguey-Zinsou, I. Michie, R.M. Dinsdale, A.J. Guwy, Z.X. Guo, G.C. Premier, Porous anodes with helical flow pathways in bioelectrochemical systems: the effects of fluid dynamics and operating regimes, J. Power Sources 213 (2012) 382–390, https://doi.org/10.1016/j.jpowsour.2012.03.040.
[26] W. He, M.J. Wallack, K.Y. Kim, X. Zhang, W. Yang, X. Zhu, Y. Feng, B.E. Logan, The effect of flow modes and electrode combinations on the performance of a multiple module microbial fuel cell installed at wastewater treatment plant, Water Res. 105 (2016) 351–360, https://doi.org/10.1016/j.watres.2016.09.008.
[27] F. Zhang, K.S. Jacobson, P. Torres, Z. He, Effects of anolyte recirculation rates and catholytes on electricity generation in a litre-scale upflow microbial fuel cell, Energy Environ. Sci. 3 (2010) 1347–1352, https://doi.org/10.1039/c001201g.
[28] D. Pant, G. Van Bogaert, M. De Smet, L. Diels, K. Vanbroekhoven, Use of novel permeable membrane and air cathodes in acetate microbial fuel cells, Electrochim. Acta 55 (2010) 7710–7716, https://doi.org/10.1016/j.electacta.2009.11.086.
[29] X. Zhang, D. Pant, F. Zhang, J. Liu, W. He, B.E. Logan, Long-term performance of chemically and physically modified activated carbons in air cathodes of microbial fuel cells, ChemElectroChem 1 (2014) 1859–1866, https://doi.org/10.1002/celc.201402123.
[30] R.D. Cusick, B. Bryan, D.S. Parker, M.D. Merrill, M. Mehanna, P.D. Kiely, G. Liu, B.E. Logan, Performance of a pilot-scale continuous flow microbial electrolysis cell fed winery wastewater, Appl. Microbiol. Biotechnol. 89 (2011) 2053–2063, https://doi.org/10.1007/s00253-011-3130-9.
[31] Y. Feng, Q. Yang, X. Wang, B.E. Logan, Treatment of carbon fiber brush anodes for improving power generation in air-cathode microbial fuel cells, J. Power Sources 195 (2010) 1841–1844, https://doi.org/10.1016/j.jpowsour.2009.10.030.
[32] Q. Yang, Y. Feng, B.E. Logan, Using cathode spacers to minimize reactor size in air cathode microbial fuel cells, Bioresour. Technol. 110 (2012) 273–277, https://doi.org/10.1016/j.biortech.2012.01.121.
[33] W. He, W. Yang, Y. Tian, X. Zhu, J. Liu, Y. Feng, B.E. Logan, Pressurized air cathodes for enhanced stability and power generation by microbial fuel cells, J. Power Sources 332 (2016) 447–453, https://doi.org/10.1016/j.jpowsour.2016.09.112.
[34] B. Wei, J.C. Tokash, F. Zhang, Y. Kim, B.E. Logan, Electrochemical analysis of separators used in single-chamber, air-cathode microbial fuel cells, Electrochim. Acta 89 (2013) 45–51, https://doi.org/10.1016/j.electacta.2012.11.004.
[35] W. Yang, R. Rossi, Y. Tian, K.-Y. Kim, B.E. Logan, Mitigating external and internal cathode fouling using a polymer bonded separator in microbial fuel cells, Bioresour. Technol. 249 (2017) 1080–1084, https://doi.org/10.1016/j.biortech.2017.10.109.
[36] B.E. Logan, B. Hamelers, R. Rozendal, U. Schröder, J. Keller, S. Freguia, P. Aelterman, W. Verstraete, K. Rabaey, Microbial fuel cells: methodology and technology, Environ. Sci. Technol. 40 (2006) 5181–5192, https://doi.org/10.1021/es0605016.
[37] R. Rossi, W. Yang, E. Zikmund, D. Pant, B.E. Logan, In situ biofilm removal from air cathodes in microbial fuel cells treating domestic wastewater, Bioresour. Technol. 265 (2018) 200–206, https://doi.org/10.1016/j.biortech.2018.06.008.
[38] B.E. Logan, E. Zikmund, W. Yang, R. Rossi, K.-Y. Kim, P.E. Saikaly, F. Zhang, Impact of ohmic resistance on measured electrode potentials and maximum power production in microbial fuel cells, Environ. Sci. Technol. 52 (2018) 8977–8985, https://doi.org/10.1021/acs.est.8b02055.
[39] Y. Ahn, F. Zhang, B.E. Logan, Air humidity and water pressure effects on the performance of air-cathode microbial fuel cell cathodes, J. Power Sources 247 (2014) 655–659, https://doi.org/10.1016/j.jpowsour.2013.08.084.
[40] S. Cheng, W. Liu, J. Guo, D. Sun, B. Pan, Y. Ye, W. Ding, H. Huang, F. Li, Effects of hydraulic pressure on the performance of single chamber air-cathode microbial fuel cells, Biosens. Bioelectron. 56 (2014) 264–270, https://doi.org/10.1016/j.bios.2014.01.036.
[41] S. Cheng, Y. Ye, W. Ding, B. Pan, Enhancing power generation of scale-up microbial fuel cells by optimizing the leading-out terminal of anode, J. Power Sources 248 (2014) 631–638, https://doi.org/10.1016/j.jpowsour.2013.10.014.
[42] S. Cheng, B.E. Logan, Increasing power generation for scaling up single-chamber air cathode microbial fuel cells, Bioresour. Technol. 102 (2011) 4468–4473, https://doi.org/10.1016/j.biortech.2010.12.104.